Warm Core Structure of Hurricane Erin Diagnosed from High Altitude Dropsondes during CAMEX-4

J. B. HALVERSON

Mesoscale Atmospheric Processes Branch, NASA Goddard Space Flight Center, Greenbelt, Maryland

J. SIMPSON AND G. HEYMSFIELD

NASA Goddard Space Flight Center, Greenbelt, Maryland

H. PIERCE

Science Systems Applications, Inc., Lanham, Maryland

T. HOCK

Atmospheric Technology Division, National Center for Atmospheric Research, Boulder, Colorado

L. RITCHIE

University of New Mexico, Albuquerque, New Mexico

(Manuscript received 7 November 2003, in final form 22 February 2005)

ABSTRACT

A combination of multiaircraft and several satellite sensors were used to examine the core of Hurricane Erin on 10 September 2001, as part of the Fourth Convection and Moisture Experiment (CAMEX-4) program. During the first set of aircraft passes, around 1700 UTC, Erin was still at its maximum intensity with a central pressure of 969 hPa and wind speed of 105 kt (54 m s^{-1}).

The storm was moving slowly northwestward at 4 m s^{-1}, over an increasingly colder sea surface. Three instrumented aircraft, the National Oceanic and Atmospheric Administration (NOAA) P3 with radar, the National Aeronautics and Space Administration (NASA) ER-2 at 19 km, newly equipped with GPS dropwindsondes, and the NASA DC-8 with dropwindsondes flew in formation across the eye at about 1700 UTC and again 2.5 h later around 1930 UTC. The storm had weakened by 13 m s^{-1} between the first and second eye penetrations. The warm core had a maximum temperature anomaly of only 11°C, located at 500 hPa, much weaker and lower than active hurricanes. The core appeared to slant rearward above 400 hPa. Even on the first penetration, airborne radar showed that the eyewall cloud towers were dying. The tops fell short of reaching 15 km and a melting band was found throughout. The tropopause had a bulge to 15.8-km elevation (environment ~14.4 km) above the dying convection.

The paper presents a consistent picture of the vortex in shear interaction from a primarily thermodynamic perspective. A feature of Erin at this time was a pronounced wavenumber-1 convective asymmetry with all convective activity being confined to the forward quadrants on the left side of the shear vector as calculated from analyses. This is similar to that predicted by the mesoscale numerical models, which also predict that such small amounts of shear would not affect the storm intensity. In Erin, it is remarkable that relatively small shear produced such a pronounced asymmetry in the convection. From the three-dimensional analysis of dropsonde data, horizontal asymmetries in lower and middle tropospheric warming were identified. The warm anomalies are consistent with the pattern of mesoscale vertical motions inferred from the shear-induced wavenumber-1 asymmetry, dipole in rain intensity, and surface convergence.

Corresponding author address: Dr. Jeffrey B. Halverson, Code 912, Mesoscale Atmospheric Processes Branch, NASA Goddard Space Flight Center, Greenbelt, MD 20771.
E-mail: halverson@agnes.gsfc.nasa.gov

1. Introduction

The structure of the tropical cyclone warm core has been the subject of numerous studies spanning decades of research. With the turn of the century, we have an improved but still incomplete understanding of hurricane structure and its evolution. The warming of the eye arises from a combination of latent heat release from condensation and freezing in intense eyewall convection together with subsidence near and within the eye itself. These processes and the factors controlling them need to be understood to improve intensity forecasts. Vertical wind shear has long been believed to inhibit storm growth, but data to understand variations in vertical winds and their impacts remain scarce.

New remote sensing technologies have suggested the importance of mesoscale processes in the storm core. Their recognition has already led to promising hypotheses that can only be advanced by closely spaced complete vertical profiles of wind, temperature, and moisture. Dropwindsonde capability was installed on two National Aeronautics and Space Administration (NASA) aircraft, the upper one flying at 20 km. Here we present results from mature Hurricane Erin (2001), the first hurricane for which these deep profiles were obtained. To glimpse the immense pioneering research that led to the present knowledge on mesoscale processes, the reader is referred to Simpson (2002).

During the past few decades, satellite microwave sounders have emerged as a new means to quantify the magnitude of the eye temperature anomaly. The coarse horizontal resolution (~40 km) usually includes part of the eyewall, so that algorithms correcting for precipitation have been difficult (Simpson 2002, chapter 11).

The Fourth Convection and Moisture Experiment (CAMEX-4) recently provided a means to infuse new observational technologies into targeted missions investigating the structure and evolution of Atlantic hurricanes. CAMEX-4 was a campaign conducted jointly by the NASA and National Oceanographic and Atmospheric Administration (NOAA) during August and September 2001. One of its novel aspects was the deployment of a new dropsonde system on the NASA ER-2 research aircraft, which overflew hurricanes at altitudes of 20 km.

The mission flown into Hurricane Erin on 10 September 2001 marked the first time that dropwinsondes were released inside the eye of a hurricane from such high altitudes. By combining the ER-2 core dropsondes with those released from the NASA DC-8, which flew within a two-degree radius of storm center, we obtained a detailed three-dimensional mapping of the warm anomaly. The complex relationship of this warming to the eyewall convective towers, vortex winds, and variations in the tropopause height across the inner core region is described for a several hour period in Erin.

In this paper, we present a detailed account of the warm core as it relates to a vertical wind shear that was beginning to interact with Erin. We will also demonstrate how Erin's surface pressure reduction can be accounted for by various vertical layers of warming within the eye. In the following section, we will describe the unique dropsonde platform employed on the ER-2 and how the dropsonde temperature profiles were used to quantify and map the eye's warm anomaly. In section 3, we present a brief history of Erin's origins and evolution with a focus on 10 September (very early weakening) and how a wavenumber-1 asymmetry developed, possibly as a result of the shear–vortex interaction. Section 4 details the three-dimensional structure of the warm core and tropopause height variation across the inner core of the storm. We will document interesting asymmetries in the thermal structure that may have arisen through the wind shear interactions described in section 3. This paper provides a unique observational snapshot of the structure of a mature Atlantic category 2 storm early in its dissipation.

2. Data and methods

The ER-2 dropsonde system, termed the Automated Advanced Vertical Atmospheric Profiling System (AAVAPS) was developed as a joint venture between the National Center for Atmospheric Research (NCAR) Atmospheric Technology Division (ATD), the NASA Dryden Flight Research Center (DFRC), and the Joint Center for Earth Systems Technology (JCET) at the University of Maryland Baltimore County. The core system utilizes the standard AVAPS used by NOAA and NASA research aircraft, now a fully automated system capable of operator-free dropsonde initialization, channel selection, ejection, telemetry reception, and data storage. Up to 16 dropsondes are deployed in a barrel-type launcher and the system allows simultaneous tracking of sondes on four separate channels. The ER-2 pilot commands a dropsonde release by merely pressing a button. The dropsonde units are modified RD-93 type models [as described in Hock and Franklin (1999)] manufactured jointly by NCAR ATD and Vaisala, Inc., and contain a full-up GPS engine for wind finding. Thermodynamic and wind data are recorded at 0.5-s intervals and a typical descent from 20.5 km takes about 23 min. Algorithms are then applied, which include dynamic corrections to account for fast fall speed during the first few minutes of descent. Typical vertical resolutions range from about 7 m

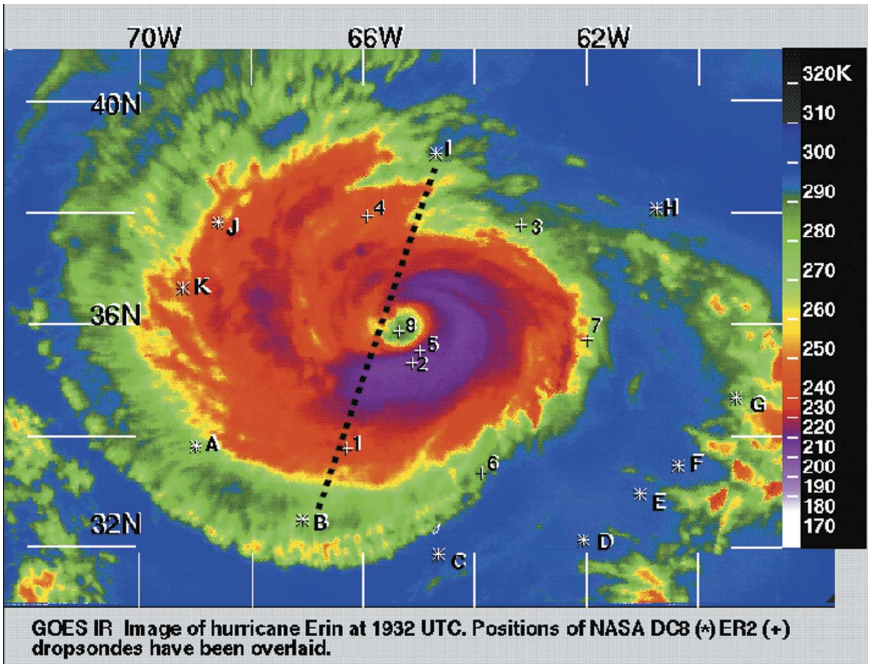

FIG. 1. Infrared snapshot of Hurricane Erin at 1932 UTC 10 Sep 2001. Cloud-top temperatures (K) are indicated by the scale on rhs. Letters refer to location of dropsondes released by the NASA DC-8; numbers indicate dropsondes released by the ER-2. ER-2 drop 8 corresponds to the center of the eye. Black dotted line is the location of the composite cross section constructed through the core using nearby dropsondes.

near the surface to 20 m at 20-km altitude. The accuracy of the sensors is ±1.0 hPa for pressure, ±0.2°C for temperature, ±0.1 m s^{-1} for wind components and ±7% for relative humidity.

The ER-2 Doppler Radar (EDOP) was also flown on the ER-2 in conjunction with the dropwinsondes. EDOP is an X-band (9.6 GHz), dual beamwidth system, described in detail in Heymsfield et al. (2001), and provides detailed vertical profiles of hydrometeor reflectivity factor beneath the aircraft flight track. EDOP cross sections of hydrometeor reflectivity factor are used in section 4 to describe the variable slope, depth, and intensity of eyewall convection in relation to the shear and warm core.

Figure 1 shows the pattern of dropsondes dropped from the NASA DC-8 and ER-2 within Erin's circulation between 1600 and 2030 UTC 10 September. The drop locations are superimposed on a false-color infrared image of Erin at 1932 UTC. The image time was chosen to coincide with a sonde release down the eye center, while Erin was translating slowly to the northwest. The NASA DC-8 circumnavigated the storm at two degrees radius in a counterclockwise direction, sampling mainly the outer rain bands and the circulation periphery. Dropwinsondes were released from heights varying between 11 and 12 km. The ER-2 flew a figure-4 type survey pattern across the inner core, releasing all sondes within one degree of center. Eight dropsondes were released, at the endpoints of three legs intersecting the core at different azimuthal angles, and within the eye, from an altitude of nearly 19 km. With the crew of the NOAA P3 aircraft providing expert guidance, a dropsonde was released at 1918 UTC down the geometric center of the eye. The very weak winds, averaging 5–10 m s^{-1} during the descent, attests to the sonde's placement near the actual center. Taken together, these 20 dropwinsonde profiles are used in subsequent sections to construct detailed analyses of the warm core magnitude, radius, symmetry, and depth.

The height variation of Erin's warm anomaly is constructed in section 4 by subtracting representative environmental values of temperature from the eye temperature profile at 1918 UTC. The choice of environmental profile was confounded by uncertainty as to which radius the storm circulation disappears or, alternatively, at which radius the environment begins. There are no clear or hard boundaries delineating this transition. After carefully examining all available dropsondes, we created a composite profile that utilizes a DC-8 dropsonde E at 1800 UTC in the clear air 610 km southeast of Erin's center, containing data from sea surface to a pressure height of 329 hPa. Above this level

we used data from ER-2 dropsonde 3 at 1731 UTC located 340 km to the northeast of center, on the edge of the central dense overcast. A comparison of the ER-2 and DC-8 dropsonde profiles below 350 hPa showed very small differences in temperature at all levels, and both profiles also closely compare with the Jordan (1958) mean sounding representative of the Caribbean hurricane season region.

In section 4, we present a distance–height (XZ) transect across the core of Erin. This section was synthesized from several dropsonde profiles forming a loose line oriented from southwest to northeast across the storm's circulation. The dropsondes included those released on the periphery of the outer circulation by the DC-8, as well as the ER-2 inner core drops sampling the southern eyewall and the 1918 UTC center drop. The dashed line in Fig. 1 shows the orientation of this composite slice. Our intent was to combine as many dropsondes as possible into the single representative slice through the storm center, in order to examine the general magnitude, shape and vertical extent of the warm anomaly, from sea surface to above tropopause height, and from the eye center to the outer circulation. Perturbation temperature values shown on the composite section were obtained after subtracting the composite ER-2/DC-8 profile at each 25-hPa level as described in the previous paragraph. No attempt was made to account for sonde drift along or outside of the analysis section. Some uncertainties may be present in this spatial analysis arising from 1) interpolation of a few sondes located a short distance off the analysis line; 2) displacement due translation of the center toward the northwest (at a rate of about 4 m s^{-1}); and 3) local temperature variations arising from storm intensity change during the three-hour aircraft mission. However, the impact of these uncertainties is probably small when one considers the larger storm-scale attributes of the warm core structure gleaned and their relationship to the general circulation and rainfall pattern.

3. Early weakening and asymmetric structure of Erin

Hurricane Erin evolved from a tropical easterly wave off Cape Verde in early September 2001. The storm was initially enshrouded in Saharan dust on 3 September and did not begin intensifying until emerging from the dust late on 7 September. At this time Erin began moving toward the northwest. Figure 2 presents a time series of maximum sustained wind and best track obtained from the NOAA Tropical Prediction Center. Rapid deepening of Erin ensued on 8 and 9 September with a peak maximum sustained wind of 105 kt (54 m s^{-1}) briefly attained by 1800 UTC 9 September. Thereafter Erin maintained this intensity level until 1200 UTC 10 September, at which point the maximum wind speed began to weaken. As the CAMEX-4 mission was flown into Erin, the storm weakened 25 kt (13 m s^{-1}) while moving toward the northwest at approximately 8–10 kt (4–5 m s^{-1}). On 11 September, a more gradual weakening commenced and the storm recurved sharply toward the east.

Our analysis of the Atlantic three-day composite sea surface temperature (SST) derived from the Tropical Rainfall Measurement Mission (TRMM) Microwave Radiometer (TMI) shows that Erin moved into sharply cooler waters late on 9 September. Located initially over 30°C water at 0000 UTC 9 September, by 1800 UTC the storm was overlying 27°C temperatures. This was the most obvious cause of Erin's sudden weakening.

As Erin crossed the temperature gradient into much cooler SSTs, the storm encountered a southerly shear of about 7–8 m s^{-1} (0000 UTC 9 September). Analyses from the Navy Operational Global Atmospheric Prediction System (NOGAPS) were used to compute a mean tropospheric shear vector, obtained by subtracting the u and v components at 850 hPa from those at 200 hPa, and averaging over a radius extending 500 km from Erin's center. The shear was being induced by strong southerly flow aloft ahead of a short wave trough in the upper level westerlies. At 1200 UTC 10 September, the trough was located off Cape Hatteras, North Carolina.

We hypothesize that the shear produced the marked asymmetry of rainfall around Erin's inner core (e.g., Fig. 3). Many model simulations show that shear excites a steady wavenumber-1 pattern in the vertical motion field with ascent on the downshear-left side of the shear vector, enhancing convection, and descent on the upshear-right side, suppressing convection. A model study by Wang and Holland (1996) shows that the asymmetric convection affects storm motion, with storm motion deflected toward the region of maximum convection. Studies by Frank and Ritchie (1999, 2001) show that strong vertical shear reduces storm intensity. Observational confirmation of these model studies requires detailed wind fields, which so far have been obtained in just a few hurricanes (Franklin et al. 1993; Reasor et al. 2000; Black et al. 2002).

With a moist mesoscale model, Frank and Ritchie (2001) predict that even weak shears on the order of 3–5 m s^{-1} can cause asymmetries in the eyewall structure. The asymmetries develop within just a few hours of the imposed shear and persist several hours. In their model, the storms weaken (i.e., undergo an increase in central pressure) with a time lag inversely related to the

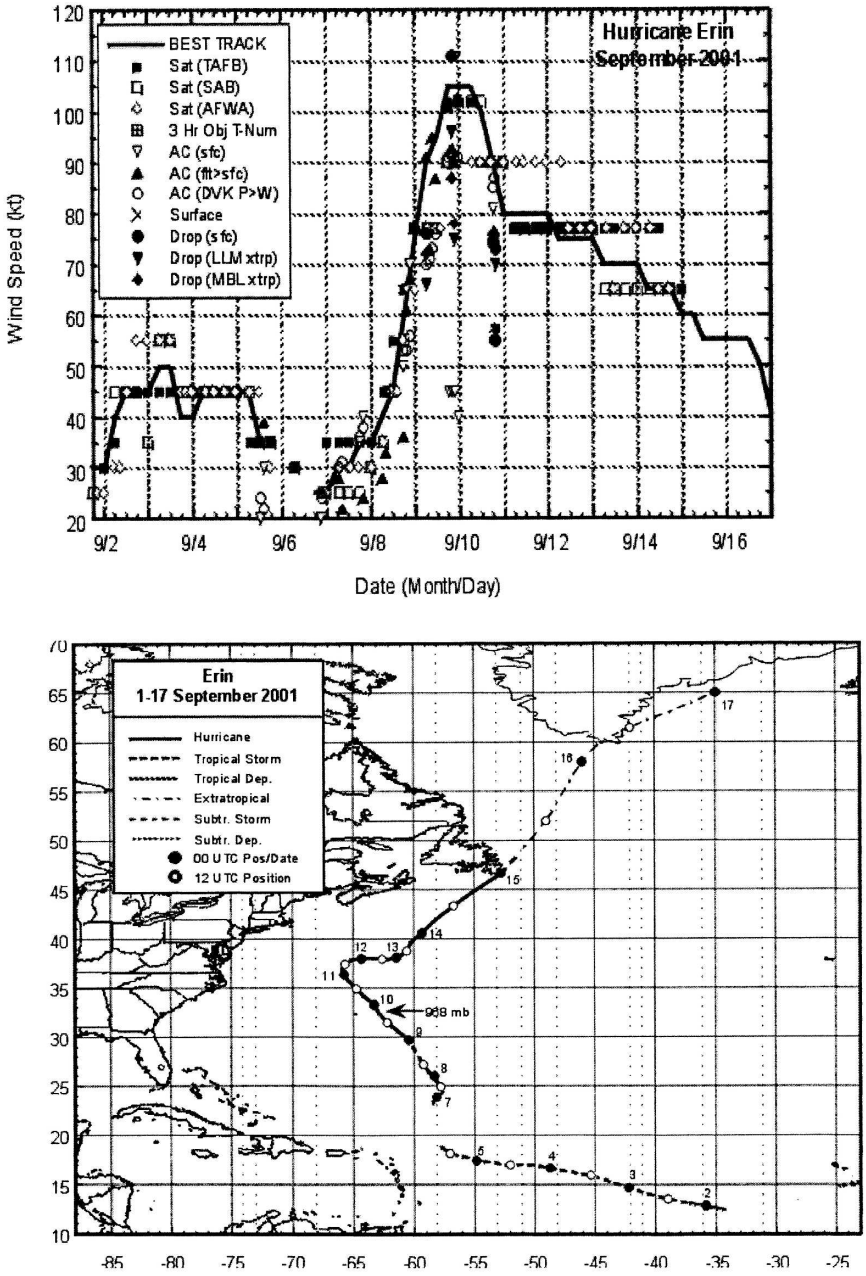

FIG. 2. (top) Maximum sustained wind (MSW) of Hurricane Erin as a function of time, obtained from NOAA Tropical Prediction Center. (bottom) The best track for Erin.

shear magnitude. This finding suggests that shear measurements may help predict hurricane intensity. Thus the Erin case provides a rare and important opportunity to test and verify model results, which could have a very important forecast impact.

Frank and Ritchie (2001) describe the chain of processes by which the shear alters and weakens their model storm. Advection by the shear produces upper-level divergence and thus low-level convergence downshear of the center. The upper-level warm core is dissipated downstream, so that the storm weakens from the top down. The helical nature of the updraft in strong hurricanes creates an azimuthal separation between direct downshear updraft initiation, and displacement of heaviest precipitation further down wind (in an azimuthal sense).

Figure 3 superimposes the 10 September deep tropospheric shear vector on the horizontal distribution of

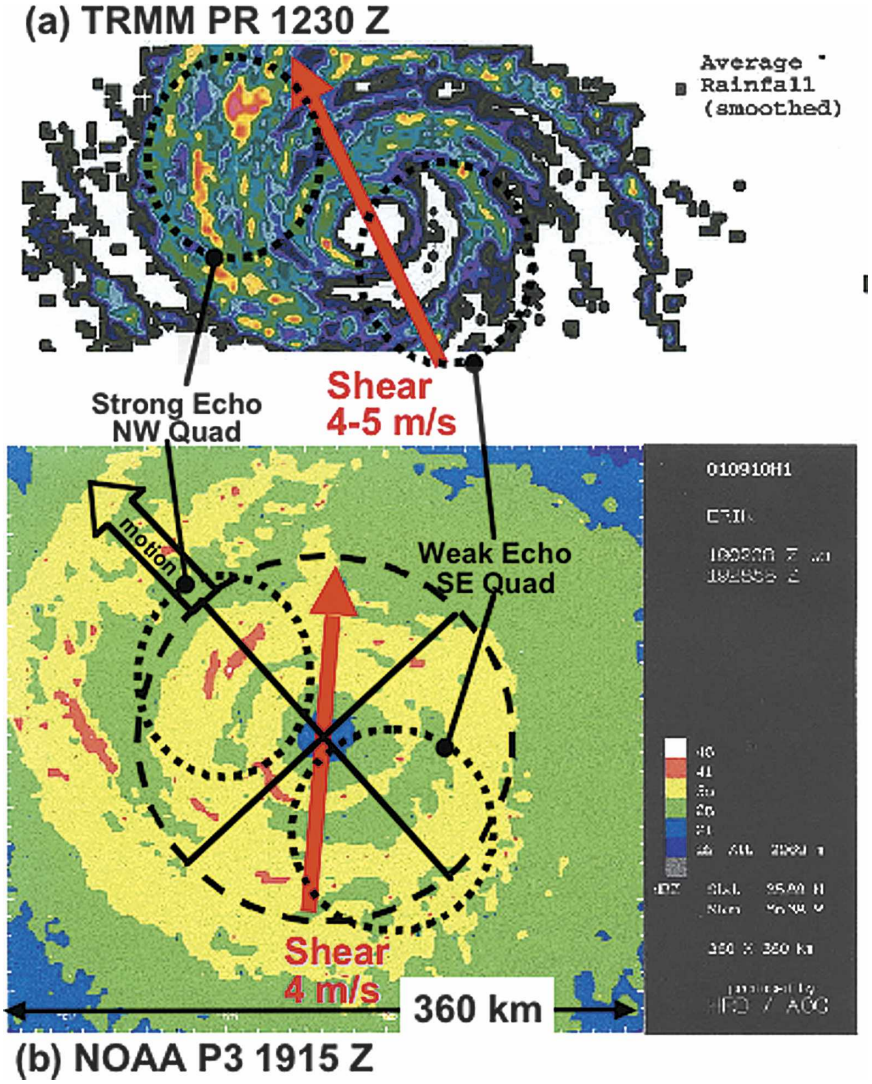

FIG. 3. (top) The surface rain distribution across Erin as measured by the TRMM Precipitation Radar on 1230 UTC 10 Sep. Orange and red regions in the western semicircle (forward quadrants) represent the largest rain rates. (bottom) The composite reflectivity factor structure of Erin measured by the NOAA P3 aircraft at 1915 UTC 10 Sep from an altitude of 4 km. Orange and white regions show the largest reflectivity factor values. In both panels, heavy dashed black circles indicate regions of greatest rainfall asymmetry. Heavy red arrow indicates the average direction of the deep tropospheric shear vector between 1200 UTC 10 Sep and 0000 UTC 11 Sep. Heavy black arrow shows direction of storm motion.

radar reflectivity factor at 1230 and 1915 UTC. The shear remained oriented from a general southerly direction with a magnitude of 4–5 m s^{-1}. Two snapshots of rain reflectivity factor are shown—one from the TRMM Precipitation Radar at 1230 UTC, and the second taken from the surveillance radar aboard the NOAA P3 aircraft radar at 1915 UTC. The largest reflectivity factor values (45–50 dBZ, both panels) occur in a rainband in the forward sector, about 100 km northwest of the center. In the eyewall, the strongest echoes appear further downwind (cyclonically). They occur in the left quadrants, southwest of the center. This asymmetric distribution of rainfall is persistent and conforms to the dipole pattern of downshear-left (upshear right) ascent (descent) that the models predict. In the TRMM image, a weak-echo region with returns less than 20 dBZ spans the rear (southeast) quadrants, and a broad reflectivity factor-free moat occurs just outside the eyewall in this same quadrant. This moat may be due to the presence of reflectivity factor values below

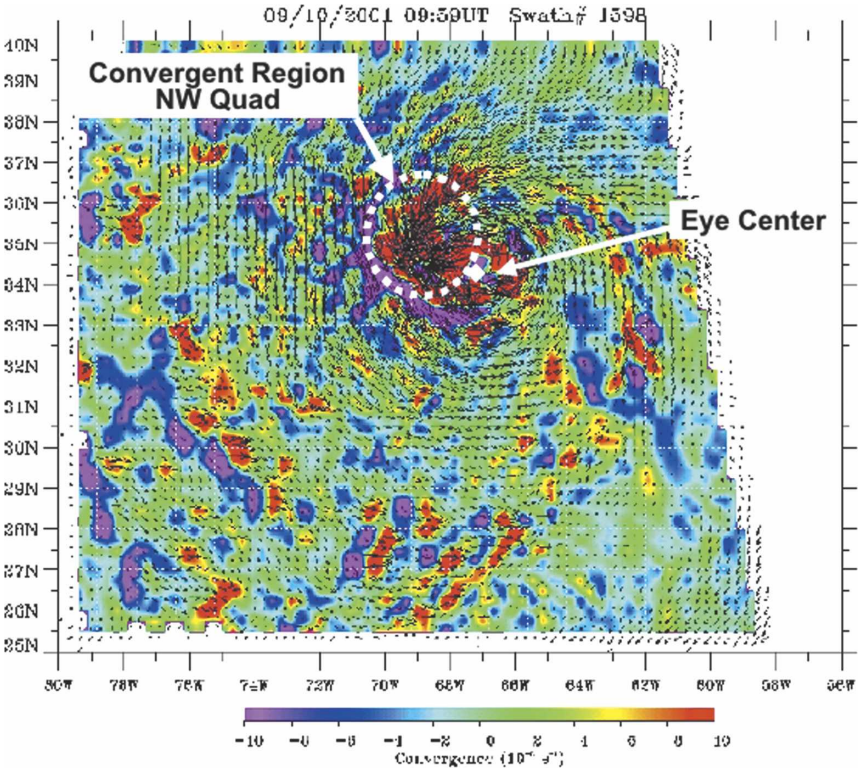

FIG. 4. Map of sea level convergence obtained from gridded QuikSCAT data, with storm motion subtracted from the winds, at 1000 UTC 10 Sep. Red areas denote convergence, and purple show divergence. The center of the eye is shown by the white diamond.

the minimum TRMM detection threshold of about 17 dB*Z*. A NASA Quick Scatterometer (QuikSCAT) overpass of Erin, taken at 1000 UTC 10 September, is shown in Fig. 4. (It is possible that heavy rain has led to some contamination of wind vectors shown in the figure.) This diagram shows the pattern of sea surface wind vectors, with mean storm motion subtracted out. Convergent areas are shown in red; peak surface convergence is found in the front (northwest) sector. A spatially coherent zone of surface convergence on the order of $-10 \times 10^{-5}\ \mathrm{s}^{-1}$ extends 100–150 km northwest of the eyewall. A coherent pattern of convergence is lacking in the southeastern or right rear quadrant of Erin. The pattern of surface forcing is thus consistent with an asymmetric pattern of low-level ascent that would produce the observed dipole in radar reflectivity factor, and is the expected pattern given the orientation of the shear vector.

Comparing Fig. 3 with Fig. 4, we note a substantial cyclonic displacement of the maximum radar echoes from the inferred low-level forcing. At 1915 UTC, the P3 radar shows that the heaviest rain echoes are located in the western semicircle/northwest (forward) quadrants, with minimal echo intensity in the eastern semicircle/southeast (rear) quadrants. In the eyewall the strong precipitation echoes are southwest of the storm center, or left quadrants relative to storm motion. The Geostationary Operational Environmental Satellite (GOES) infrared image, however, shows that the maximum cloud-top heights are displaced still further downwind (cyclonically) than the radar echoes. In the southeastern (rear) quadrants, brightness temperature values are as low as −65°C. The P3 radar scan, taken within minutes of the GOES image, implies that the area of tall cloud tops must be the deepest remnants of earlier, more vigorously precipitating echoes that grew and matured in the western (forward) sectors. Thus, by comparing the QuikSCAT, TRMM, NOAA P3 radar, and GOES information, one hypothesizes that a pattern of asymmetric ascent was being established by interaction between the hurricane vortex and shear. New cells form in the northwest (forward) sector, rapidly grow, rain out, and dissipate as they propagate or are advected cyclonically around to the rear side of the storm (southern semicircle). In the right rear (southeast) quadrant, the shear–vortex interaction has probably established some degree of subsidence throughout the middle and lower troposphere, causing the weakening or dissipation of rain cores.

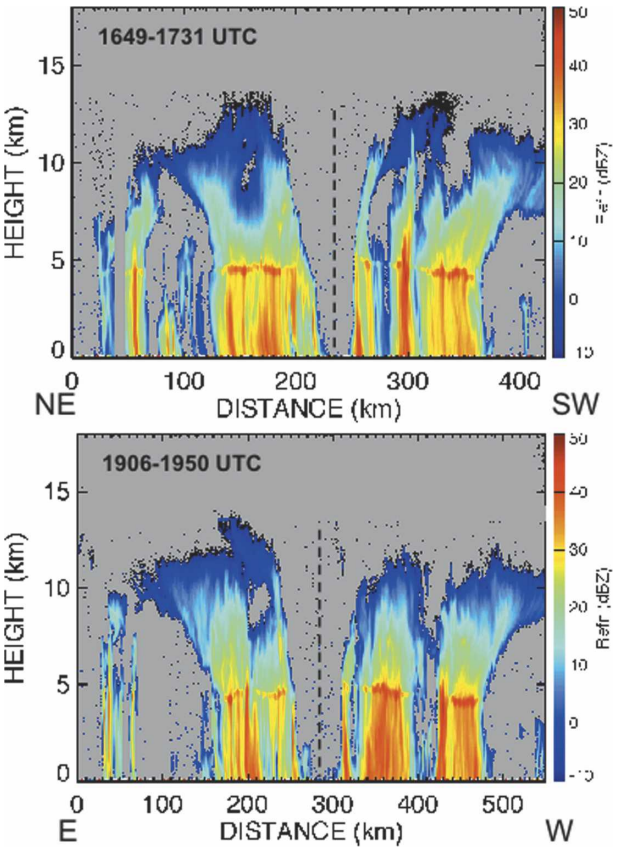

FIG. 5. Height–distance cross sections through Erin's core showing radar reflectivity factor, provided by the nadir-viewing EDOP. (top) A northeast-to-southwest slice from 1649 to 1731 UTC; (bottom) an east–west transect from 1906 to 1950 UTC. Range of reflectivity factor values is shown by scale on the right. Vertical dashed line shows approximate location of vortex axis if it were vertically erect, for reference.

Figure 5 shows two vertical scans across Erin's inner core taken by the EDOP. A west-to-east-oriented scan is shown in the bottom panel, between 1906 and 1950 UTC, and a scan from southwest to northeast is shown in the top panel, from 1649 to 1731 UTC. There is a component of northerly eyewall tilt in the 1649–1731 UTC section. The southern eyewall remains erect while the northern side slopes strongly toward the north, in agreement with the sense of the deep tropospheric shear. Maximum echo-top heights are generally 13 km and the radius of the eyewall is estimated to be 25 km. By contrast, in the east–west plane (roughly orthogonal to the orientation of the shear), Erin's eyewall remains fairly erect and symmetric on both sides. Aside from variations arising from sampling issues, the convection during the later ER-2 crossing is shallower (10–11-km maximum echo-top heights). The weakening of Erin's convective towers is a direct indication of the storm's decrease in strength over the ensuing two to three hours between these two ER-2 overflights.

4. Structure of Erin's warm core

In the foregoing section we discussed apparent reasons for the asymmetry in rainfall, convergence and cloud-top patterns in dissipating Hurricane Erin. This section will examine structural details of the warm anomaly within Erin's core late on 10 September. The dropsondes sampled the inner core with sufficient horizontal resolution to capture the geometry and magnitude of the storm's warm anomaly, as well as variations in tropopause height across the inner core and asymmetries in the thermodynamic fields.

Figure 6 presents a vertical slice through Erin, showing the composite structure of the warm anomaly across a line including dropsondes B (DC-8), 1, 2, 8, 4 (all taken from the ER-2), and I (DC-8). The vertical and horizontal extent of the warm core is shown in its entirety. The warming is greatest near 500 hPa with a maximum perturbation temperature value of +11°C. The warm temperatures spread horizontally with increasing height. As Fig. 7 shows, the highest values of +9° to +10°C are maintained through a deep layer from 300 down to 750 hPa. These results are broadly consistent with earlier findings such as Hawkins and Imbembo (1976). The upper limit of the warm core is 110 hPa and the tropopause is pushed upward over the eyewall and the eye (discussed later in this section). Above 200 hPa, because of the linear nature of the pressure coordinate in Fig. 7, the vertical gradient of temperature appears very large, but in fact is only on the order of 2°C km^{-1}. For comparison, Fig. 7 also presents a skew T–log p diagram showing the temperature profile in the eye center compared to the composite or environmental profile described in section 2.

The Erin warm core is contrasted with a vertical cross section of temperature anomaly analyzed in intense Hurricane Inez (1966) in Fig. 8 (Hawkins and Imbembo 1976). The Inez section was constructed from aircraft transects at five levels after a period of rapid deepening, when the storm's minimum central pressure was 927 hPa. Inez was a much more intense system compared to Erin, whose minimum central pressure increased from 970 to 974 hPa during the CAMEX-4 mission. Figure 8 shows that the great vertical depth of Inez's warm core is no different from that of Erin. However, the magnitude of the temperature anomaly in Inez is much larger (+16°C) and is found substantially higher in the troposphere (250 hPa). The Inez warm core is also narrower at the level of maximum warming; the +7°C anomaly is about 100 km across, compared to 160 km in the case of

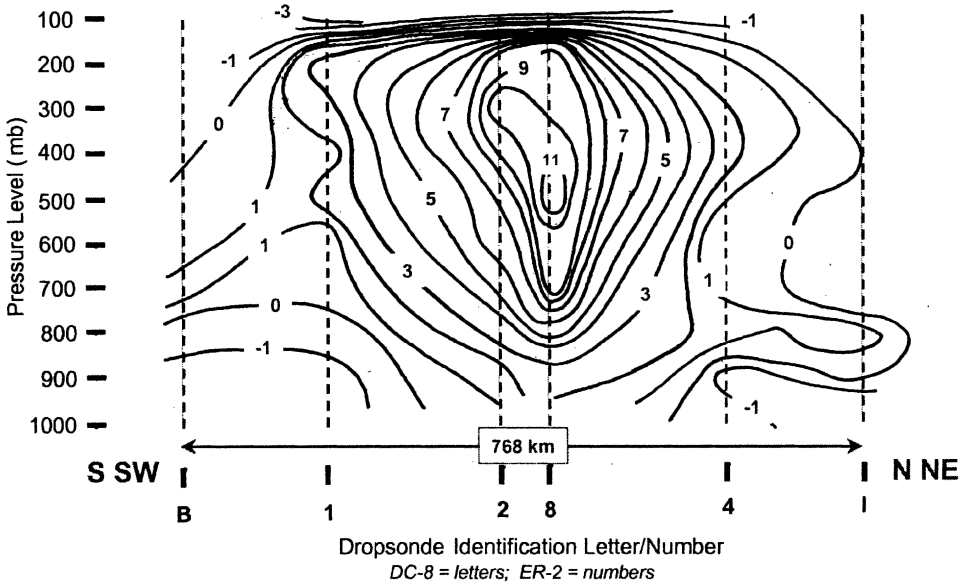

FIG. 6. Cross section through Erin's core showing temperature perturbation. Analysis was made by compositing dropsondes along/nearby the dashed line shown in Fig. 1. The vertical slide is oriented from southwest to northeast. Maximum perturbation temperature of +11ºC and distance scale are shown. Initial release times of dropsondes are 1629, 1648, 1704, 1750, 1928, and 1936 UTC for B, 1, 2, 4, 8, and I, respectively.

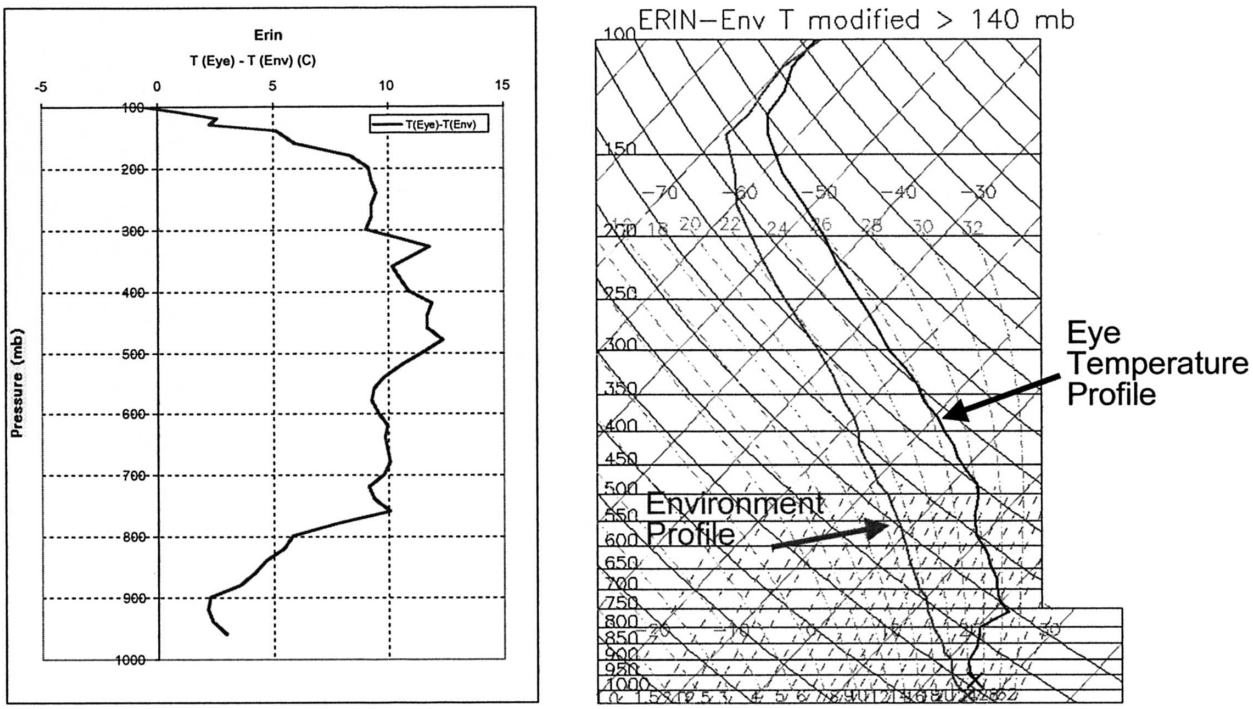

FIG. 7. (left) A vertical profile of perturbation temperature (anomaly temperature) through Erin's eye, in Cartesian coordinates. (right) Comparison of the eye temperature profile to an environmental profile in standard skew T–log$p$ format. Both sets of profiles were based on an eye dropsonde released at 1918 UTC.

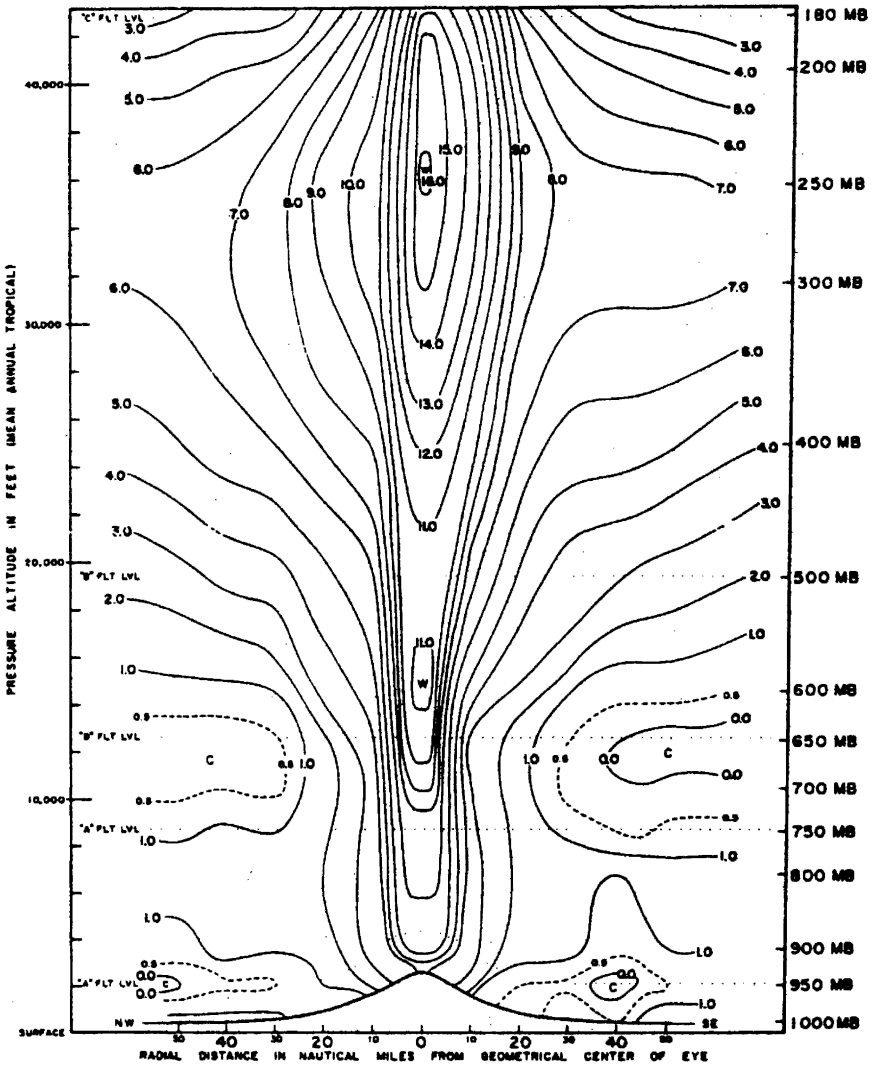

FIG. 8. Vertical section through the inner core of Hurricane Inez, showing isolines of perturbation temperature, based on aircraft transects. Figure reproduced from Hawkins and Imbembo (1976).

Erin. It is difficult to ascertain whether the broader horizontal warm core in Erin is a symptom of simultaneous weakening and spreading of the eye with time, or whether the size differences merely reflect differences in inherent diameter of the two systems.

Inez was also a much more intense storm, and the larger warming magnitude in the upper troposphere is consistent with a greater reduction in surface pressure. Table 1 shows the height in meters of the pressure levels in both the Erin environment and the eye sounding. The right-hand-side column shows how much of the pressure drop is due to warming of the layer above the particular pressure, assuming that hydrostatic conditions apply inside the eye. The 100-hPa surface differs very little in height between the environment and the eye, but is slightly higher in the eye. The main point is that the concentration of the warming producing the pressure drop is not as significant in the layers above 300 hPa [as, e.g., in moderate Hurricane Daisy, as studied by Riehl and Malkus (1961)]. In Daisy, the warming above 300 hPa contributed 47% of the pressure drop, in contrast to only 29% in Erin.

The relatively weak pattern of upper tropospheric warming in Erin is consistent with modeling results of a storm weakening from the top down. However, Erin was encountering markedly reduced SSTs at the same time as the shear set in. The reduction in SSTs translates into reduced oceanic fluxes of sensible and latent heat, weakening of eyewall convection (shown in Fig. 5) and reduced transports of high equivalent potential

TABLE 1. Percent contribution of surface pressure fall due to layer warming in eye.

Pressure (hPa)	Height environment (m)	Height eye (m)	Difference (m)	Percent difference (%)
900	1085.7	637.0	448.7	
700	3210.3	2818.7	391.6	87
500	5915.2	5626.0	289.2	64
300	9707.3	9578.2	129.1	29
200	12 432.8	12 405.8	27	6
100	16 691.6	16 706.6		

temperature into the upper troposphere. Without deeply penetrating hot towers, the warm anomaly must weaken. But as the skew *T* diagram in Fig. 7 suggests, some of the low-midlevel tropospheric warming is probably still being maintained by intense subsidence inside the eye (note the strong inversion present between 760 and 800 hPa).

In Fig. 9 we examine the structure of the warm core from a different perspective. This analysis presents isotherms of perturbation temperature made on horizontal constant pressure surfaces at five different levels (850, 600, 500, 350, and 250 hPa), stacked vertically to provide a quasi-3D view. Two quasi-vertical lines thread through common points on these surfaces. A yellow line traces the axis of nearly calm azimuthal winds in the center of the hurricane vortex, as sampled by the ER-2 dropsonde released in the eye center at 1918 UTC. A second red line passes through the centroid of the warm anomaly at each level. The temperature line is not vertically erect, lacking coincidence with the vortex center at lower levels. At 500 hPa and below, the thermal center is located northwest of the vortex axis; the central closed (perturbation) isotherm lies almost completely outside the vortex axis. At 350 hPa, the thermal centroid exactly coincides with the vortex center, and at 200 hPa both axes diverge slightly but the storm center still remains within the innermost temperature isotherm. The off-center heating maximum below 500 hPa coincides with the region of heaviest rainfall generation in the northwestern (forward) quadrants. Here, the most vigorous convective towers first develop and then travel around the western semicircle. The location of the maximum heating gradient within the region of heaviest rainfall implies generation of warming by condensational latent heat release in cells of active convection in the low layers. Numerous studies have demonstrated that the convective heating peak is normally a maximum between 3 and 5 km (Tao et al. 2001), well within the layers below 500 hPa shown in Fig. 9. The local production of heaviest rain cells in the northwest (forward) quadrants of Erin may have been

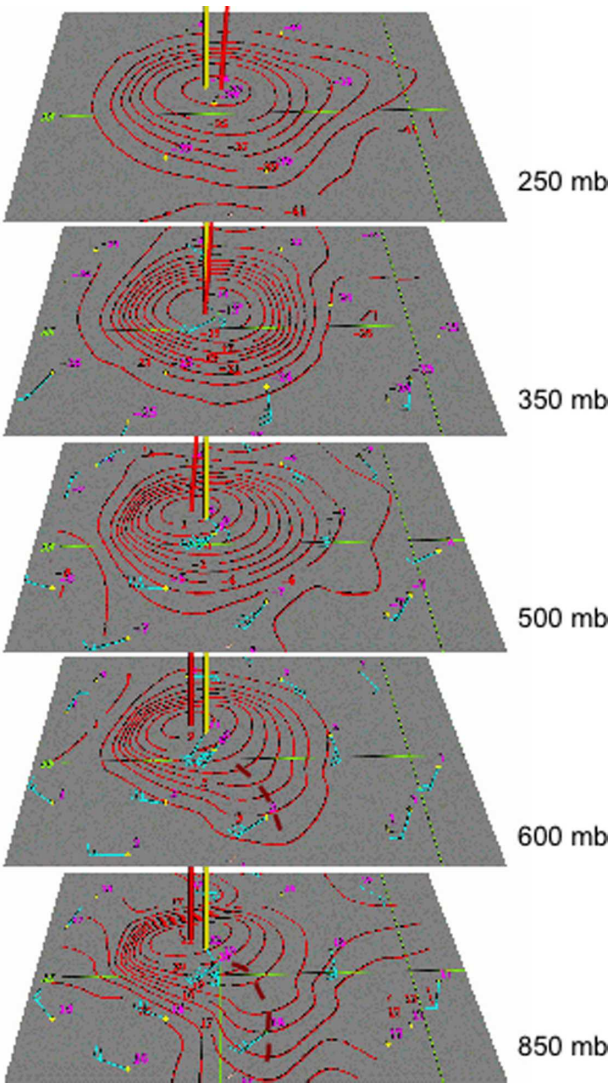

FIG. 9. Horizontal distribution of temperature within Erin's inner core at five different analysis levels (250, 350, 500, 600, and 850 hPa). The analysis makes use of all high-altitude dropsonde data from the NASA DC-8 and ER-2. Dropsonde locations are shown with yellow +. Wind barbs (kt) are shown in blue. Temperature values of each dropsonde and isotherms are shown in red. Heavy red dashed lines at 600 and 850 hPa point out an extension of the low-level warm core to the southeast. Solid yellow vertical line passes through the wind vortex center at all levels; solid red vertical line passes through the centroid of the innermost closed isotherm at each level.

sufficient to cause the asymmetry in the eye's distribution of temperature. Even during dissipation, convective clouds continue to maintain a warm anomaly at these lower levels.

A second and more pronounced asymmetry occurs in the warm core below 500 hPa. At the 600- and 800-hPa analysis levels, the warm core forms an elongated thermal ridge to the southeast of the vortex center (shown

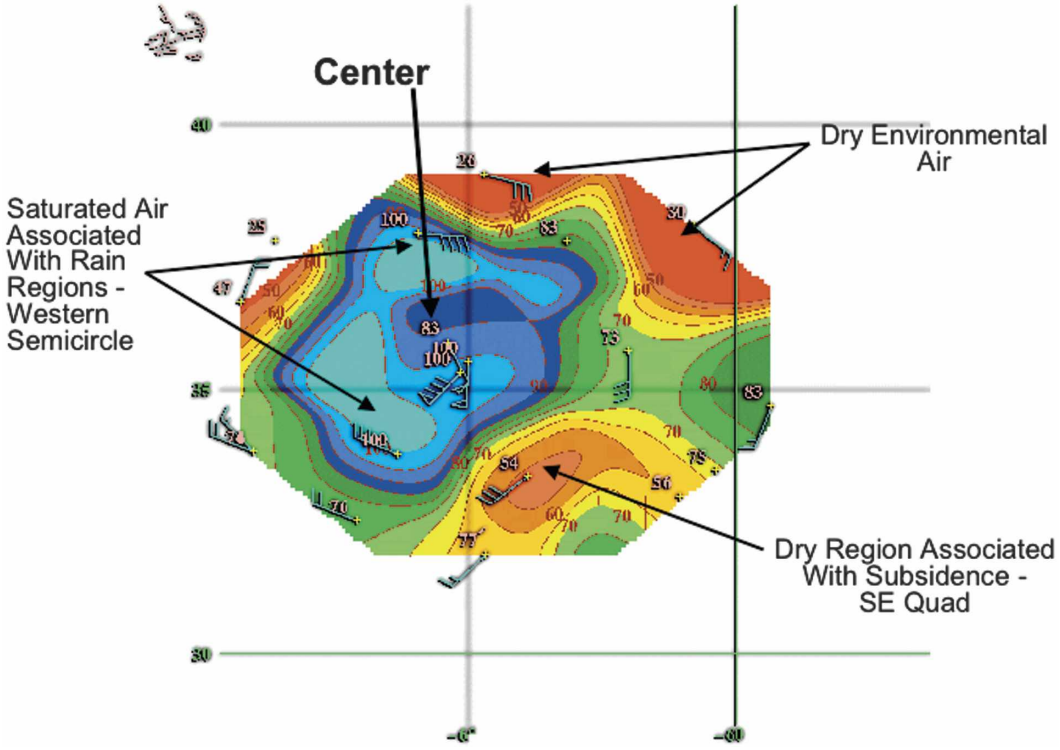

FIG. 10. Analysis of relative humidity (%) at the 850-hPa level through Erin's inner core, using all NASA DC-8 and ER-2 data. High humidity values are shown by the blue contour color fills; dry values are shown in orange and red tones. Dropsondes locations are shown by white +, and relative humidity values of each dropsonde location are shown in white.

by the dashed maroon line in Fig. 9). The extension of warming southeast of center may be an indirect consequence of the deep tropospheric shear. Observational and modeling studies have shown that the shear–vortex interaction induces subsidence upshear and to the left of the shear, primarily in the lower troposphere (Franklin et al. 1993; Frank and Ritchie 2001). The enhanced warming in the southeast (rear) quadrants may result from this mechanism. Sinking air in this region is also implied by the distribution of rainfall shown in Fig. 3, which reveals a persistent weak echo region just southeast of the eyewall (rear quadrants). Figure 10 shows the horizontal distribution of relative humidity at 850 hPa, analyzed from all available dropsonde data. This level was chosen to coincide with the level of maximum asymmetry in inner core warmth. Here we see saturated air around the western semicircle (left side) of the eyewall and outer rainband, where the heaviest rainfall is generated. Dry air with relative humidities below 40% intrudes around the periphery of the storm circulation in the northern quadrant suggesting that the tropical cyclone is moving into much drier environmental air. Also there is an isolated pocket of drying in the right rear (southeast) quadrant. Here relative humidity values of 50% and less are surrounded by much larger values. The vertical profile of temperature and humidity in the southeast quadrant (drop 6 in Fig. 1) reveals a dry, warm inversion layer is present at 850 hPa. The equivalent potential temperature (θ_e) value of 330 K associated with this inversion layer was compared with the vertical θ_e profile located immediately upstream (drop C in Fig. 1). Similar values of 330 K are found in two layers located above 850 mb (one at 750 mb and the other at 550 mb) and could thus serve as source regions for sinking air. The isolated nature of the dry air pocket and its coincidence with a region of minimal rainfall and anomalously warm temperatures at 850 hPa strongly suggest that air must be subsiding in this region of the storm.

In Fig. 11, the horizontal variation of tropopause heights across Erin late on 10 September is superimposed on the infrared cloud-top temperature distribution. The tropopause was defined as the height at which the temperature gradient suddenly became isothermal or nearly so. The tropopause is observed to dome broadly upward across the warm core, by about 0.6 km relative to the core's periphery. This is a hydrostatic response to the net warming of the tropospheric col-

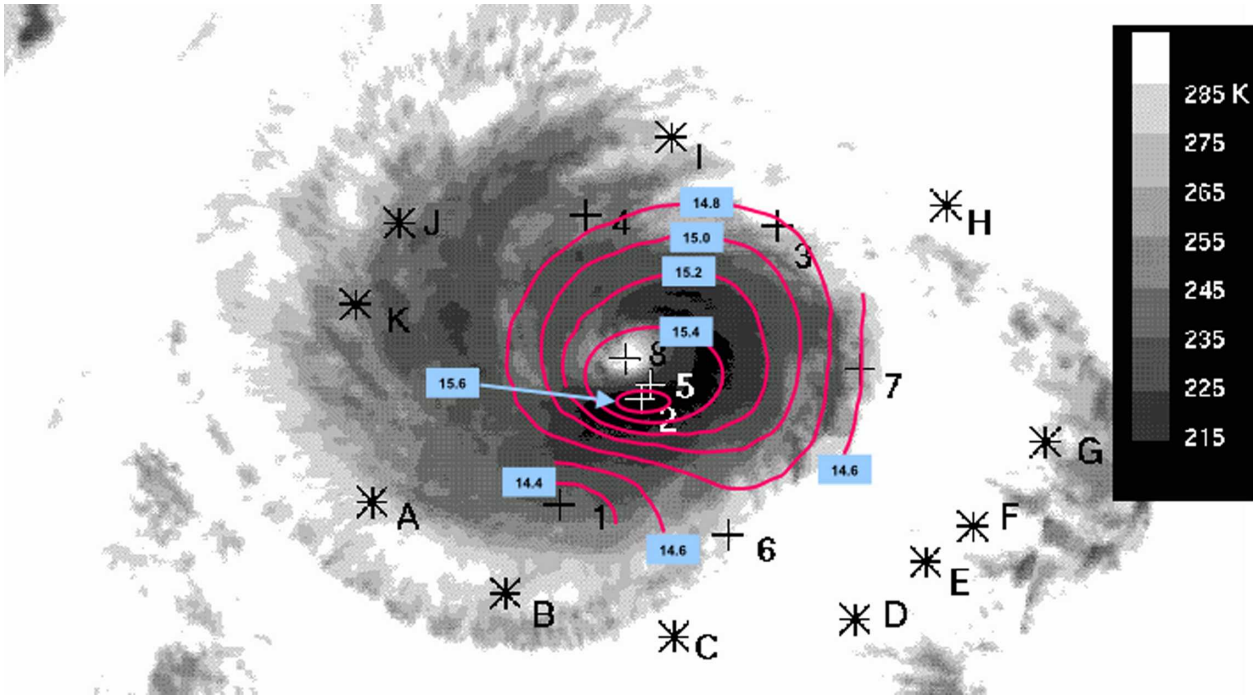

FIG. 11. Horizontal distribution of tropopause heights, obtained from ER-2 dropsonde data, superimposed on an infrared image of Hurricane Erin at 1932 UTC 10 Sep. Dropsondes are located by the black +. Red contours show the tropopause height analysis. Infrared cloud-top temperature (gray shade) is shown by the scale on the right.

umn within the eye and eyewall as shown in Fig. 10. However, the asymmetry of the upper-level warm core is also reflected in the tropopause variation. The deepest tropopause, found at 15.6 km, is located above the tallest (coldest) cloud tops in the rear quadrants, to the south and southeast of Erin's vortex center. Higher, stronger tower must have occupied that relative location earlier to raise the lid by overshooting. Little evidence of strong convection is seen in the top panel of Fig. 5. Three hours later, in the bottom panel, convective towers are replaced by the bright band, with no tops up to 15 km.

5. Summary and conclusions

Figure 12 provides a schematic summary of the inner core structure of Erin synthesized from the various aircraft and satellite observations collected late on 10 September. We found substantial asymmetry in Erin's core as did the preceding observational studies of three hurricanes with much larger vertical wind shear (Franklin et al. 1993; Reasor et al. 2000; Black et al. 2002). Pronounced asymmetry is shown in the horizontal fields of radar reflectivity factor, inner core warming, humidity, and tropopause height variations, even though the prevailing shear is relatively weak. These quantities assume the form of a dipole, which straddles the deep tropospheric shear vector. Although mesoscale vertical velocities were not actually measured across Erin, the observations paint a coherent picture consistent with theoretical and modeling studies: Downshear and to the left of the deep tropospheric shear (forward quadrants), where the shear vector is oriented from south to north, there is strong surface convergence (observed in QuikSCAT). This implies rising motion in the lower levels, and enhanced rainfall generation (observed in TRMM and the NOAA P3 radars). Where there is heavy rain, it follows that latent heating will be most intense, which may explain why the strongest warming below 500 hPa is slightly offset to the northwest of center.

On the upshear side of the deep shear vector, and to its left (southeastern sector), there is weak surface divergence, minimal rainfall, and equatorward extension of the warm core at low levels. There are two areas of strong drying. The low relative humidity on the northeast side of the core shows the effect of ventilation by outside air. The isolated, low relative humidity in the southeast probably has a different origin. It is highly likely, given the nature of the vortex–shear interaction, that adiabatic descent in the lower layers enhanced the thermal anomaly and reduced the relative humidity in this location. Meanwhile, the time required for deep

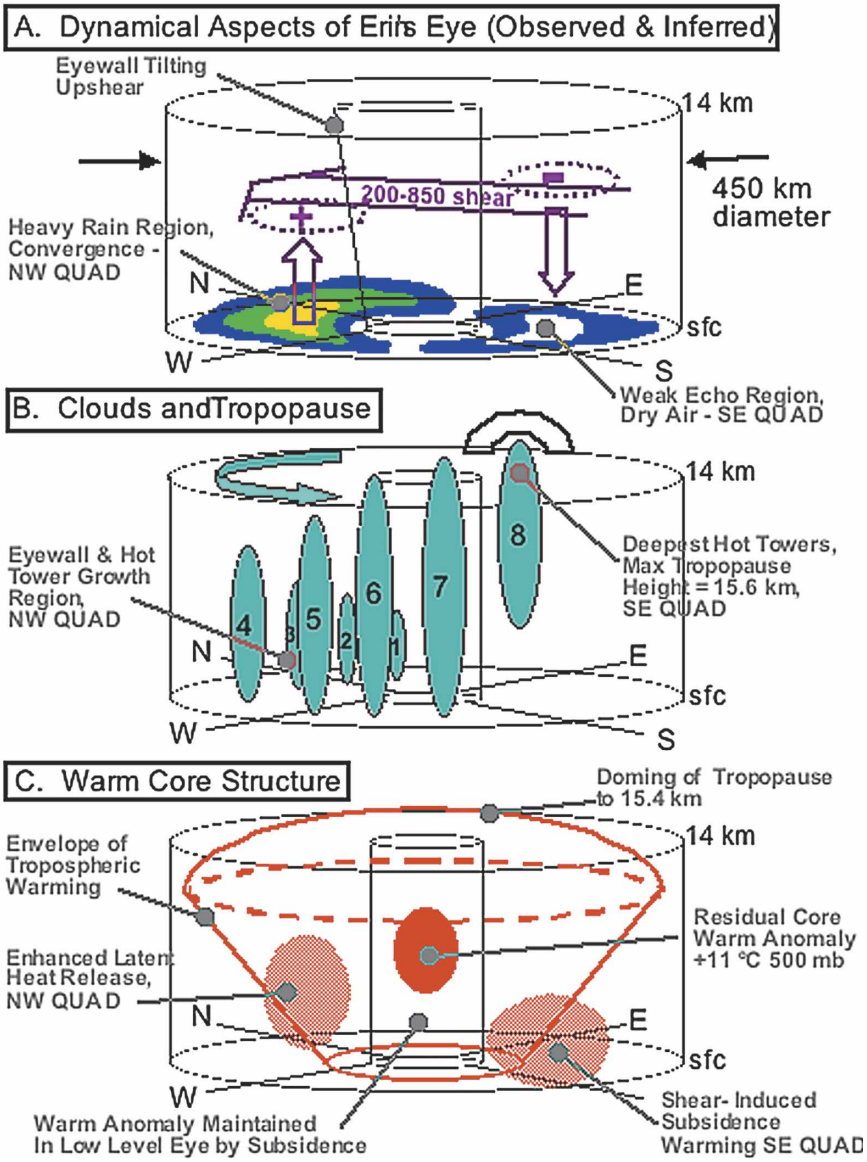

FIG. 12. Schematic synthesizing dropsonde, aircraft, and satellite observations on the structure of Hurricane Erin's inner core. (a) The relationship of shear to the rainfall distribution and hypothesized vertical motions. (b) The evolution of eyewall hot towers and tropopause height anomaly. (c) The general warm core structure and asymmetrics in the warming that are hypothesized to arise from the vortex–shear interaction.

convective growth coupled with advection of convective elements by the swirling wind place the high cold convective towers in the southeastern (rear) quadrants; here, inactive or dissipating rain clouds dominate the lower and middle troposphere (see Fig. 5). Clouds in this location relative to storm center probably attained their greatest vertical extent and raised the tropopause level to its highest elevation prior to these observations. In addition, the typical vertical couplet of mesoscale ascent (descent) operating above (below) the melting level within the stratiform regions of mesoscale convective systems (MCSs) may contribute to the observed asymmetry noted in Erin's surface wind convergence, rainfall, and thermal anomaly fields around the eye.

The sequence of events described by this combined dataset fits the scenario that Ritchie and Frank (2001) derived from their mesoscale model. A major question is how a weak shear produces such large asymmetries. The dry, barotropic vortex results of Reasor and Montgomery (2004) suggest the vortices should be extremely

resilient to even moderately large (10 m s^{-1}) amounts of shear, although it is not clear whether their vortices weakened during the integration. The moist results of Frank and Ritchie (2001) indicate the modeled tropical cyclones may weaken in relatively low shears after several days. However, many hurricanes survive much larger shears without weakening. However, Erin was moving over colder water, which by itself would cause it to weaken and dissipate. We believe that the loss of the upper-level warm core and consequent rise of the surface pressure weakened the vortex. The weaker vortex is more vulnerable to relatively low shear. The Erin study provides support for the model and shows what observations are necessary for further verification. Since the asymmetries affect both the track and intensity of hurricanes, additional high resolution datasets are required, particularly at earlier stages of the life cycle.

It is clear that the magnitude of the shear does not provide a straightforward predictive tool. The shear interacts nonlinearly with the thermal field, particularly the temperature of the upper ocean. With a warm ocean, the sea–air fluxes can sustain deep penetrative convection despite strong shear. The next generation of models will be able to simulate an interactive ocean layer. The innate three-dimensional nature of the storms will demand a large computational facility. A more serious obstacle is the lack of knowledge of the exchange coefficients in high wind speeds, where the effects of sea spray must be taken into account. Hope for flux measurements in higher winds than presently achieved in the Tropics (~20 m s^{-1}) is offered by small unoccupied airborne vehicles (UAV). It is unlikely, however, that any aircraft can survive and maintain anything like level flight under the active eyewall clouds even in a category 1 hurricane (33 m s^{-1}).

This study illustrates the importance of mesoscale measurements of key variables to develop the physical basis needed to predict hurricane intensity. Vortex–shear interactions occur on the mesoscale, as does most of the inflow and outflow. Wind profiles in the storm core and nearby surroundings are required to understand the dynamics of the wavenumber-1 asymmetries. A high-level UAV equipped with GPS dropsondes, together with remote cloud and rain measurements is needed in order to have long enough duration on station to detect changes in intensity in relation to the nearby environment.

These observational results, together with those of a similar, even more detailed observational study of a very intense hurricane (Franklin et al. 1988, 1993), provide enough support for the mesoscale models to try preliminary forecast applications. There appear to be two promising directions. Regarding intensity changes, the high-level warm core responds to the combined effect of sea surface temperature and wind shear before the low-level vortex changes intensity. The upper part of the warm core can be monitored remotely by passive microwave sounders. Until adequately high resolution sounders can be flown in space, instrumented UAVs might be cost effective. Regarding precipitation: As the storm approaches landfall, the models and present observations suggest that heavier rain should occur on the left of the shear vector. The tropospheric wind shear occurs on the regional or larger scale so that it is predicted by current global circulation models. It remains to be seen whether these predictions are good enough to be useful.

In a companion paper to this one, Heymsfield et al. (2005) document the vertical precipitation and kinematic structure of a highly sheared tropical cyclone also observed during CAMEX-4. Strong asymmetries in the pattern of rainfall, tropospheric warming and environmental factors are also found in that storm, which failed to intensify into a category 1 hurricane.

Acknowledgments. The authors gratefully acknowledge the generous support of Dr. Ramesh Kakar's CAMEX field program. We thank Drs. Robbie Hood, Edward Zipser, and Frank Marks Jr. for their expert guidance of aircraft and making the field phase a success. The authors wish to thank Richard Wohlman, Dr. Biswadev Roy, and Dr. Arlene Lang for their competent and patient operation of the DC-8 dropsonde system. Dean Lauritsen and Earle Korn of NCAR ATD provided expert technical support of dropwindsonde systems in the field. Finally, the authors graciously acknowledge the expert assistance of Dr. Robert Simpson in helping to prepare this manuscript.

REFERENCES

Black, M. L., J. F. Gamache, F. D. Marks Jr., D. E. Samsury, and H. E. Willoughby, 2002: Eastern Pacific Hurricanes Jimena of 1991 and Olivia of 1994: The effect of vertical wind shear on structure and intensity. *Mon. Wea. Rev.,* **130,** 2291–2312.

Frank, W. M., and E. A. Ritchie, 1999: Effects on environmental flow upon tropical cyclone structure. *Mon. Wea. Rev.,* **127,** 2044–2069.

——, and ——, 2001: Effects of vertical wind shear on the intensity and structure of numerically simulated hurricanes. *Mon. Wea. Rev.,* **129,** 2249–2269.

Franklin, J. L., S. J. Lord, and F. D. Marks Jr., 1988: Dropwindsonde and radar observations of the eye of Hurricane Gloria. *Mon. Wea. Rev.,* **116,** 1237–1244.

——, ——, S. E. Feuer, and F. D. Marks Jr., 1993: The kinematic structure of Hurricane Gloria (1985) determined by nested analyses of dropwindsonde and Doppler radar data. *Mon. Wea. Rev.,* **121,** 2433–2451.

Hawkins, H. F., and S. M. Imbembo, 1976: The structure of a small, intense Hurricane—Inez 1966. *Mon. Wea. Rev.,* **104,** 418–442.

Heymsfield, G. M., J. B. Halverson, J. Simpson, L. Tian, and T. P. Bui, 2001: ER-2 Doppler radar investigations of the eyewall of Hurricane Bonnie during the Convection and Moisture Experiment-3. *J. Appl. Meteor.,* **40,** 1310–1330.

——, ——, E. Ritchie, J. Simpson, J. Molinari, and L. Tian, 2006: Structure of highly sheared Tropical Storm Chantal during CAMEX-4. *J. Atmos. Sci.,* **63,** 268–287.

Hock, T., and J. L. Franklin, 1999: The NCAR GPS dropwindsonde. *Bull. Amer. Meteor. Soc.,* **80,** 407–420.

Jordan, C. L., 1958: Mean sounding for the West Indies area. *J. Meteor.,* **15,** 91–97.

Reasor, P. D., and M. T. Montgomery, 2004: A new look at the problem of tropical cyclones in vertical shear flow: Vortex resiliency. *J. Atmos. Sci.,* **61,** 3–22.

——, ——, F. D. Marks Jr., and J. F. Gamache, 2000: Low wave number structure and evaluation of the hurricane inner core observed by airborne dual Doppler radar. *Mon. Wea. Rev.,* **128,** 1653–1680.

Riehl, H., and J. Malkus, 1961: Some aspects of Hurricane Daisy, 1958. *Tellus,* **13,** 181–213.

Simpson, R. H., Ed., 2002: *Hurricane! Coping with Disaster*. Amer. Geophys. Union, 360 pp.

Tao, W.-K., and Coauthors, 2001: Retrieved vertical profiles of latent heat release using TRMM products for February 1998. *J. Appl. Meteor.,* **40,** 957–982.

Wang, Y., and G. J. Holland, 1996: The beta drift of baroclinic vortices. Part II: Diabatic vortices. *J. Atmos. Sci.,* **53,** 3737–3756.